Past and future wheat yield losses in France's breadbasket

Rogério de Souza Nóia Júnior, Pierre Martre, Jean-Charles Deswarte, Jean-Pierre Cohan, Marijn van der Velde, Heidi Webber, Frank Ewert, Alex C Ruane, Tamara Ben-Ari, Senthold Asseng

Field Crops Research 322 (2025) 109703

Contents lists available at ScienceDirect

Field Crops Research

journal homepage: www.elsevier.com/locate/fcr

Past and future wheat yield losses in France's breadbasket

Rogério de S. Nóia-Júnior [a,b], Pierre Martre [b], Jean-Charles Deswarte [c], Jean-Pierre Cohan [d], Marijn Van der Velde [e], Heidi Webber [f,g], Frank Ewert [f,h], Alex C. Ruane [i], Tamara Ben-Ari [j], Senthold Asseng [a,*]

[a] Technical University of Munich, School of Life Sciences, Department of Life Science Engineering, Chair of Digital Agriculture, HEF World Agricultural Systems Center, Freising, Germany
[b] LEPSE, Univ Montpellier, INRAE, Institut Agro Montpellier, Montpellier, France
[c] ARVALIS, Villiers-le-Bâcle, France
[d] ARVALIS, Loireauxence, France
[e] European Commission, Joint Research Centre, Ispra, Italy
[f] Leibniz-Centre for Agricultural Landscape Research (ZALF), Müncheberg, Germany
[g] Brandenburg Technical University (BTU), Cottbus, Germany
[h] Crop Science Group, INRES, University of Bonn, Bonn, Germany
[i] NASA Goddard Institute for Space Studies, New York, NY, USA
[j] UMR Innovation et transformation des sytèmes agricoles et alimentaires, INRAE, CIRAD, Institut Agro, Université de Montpellier, Montpellier, France

ARTICLE INFO

Keywords:
Compounding factors
Extreme weather
Machine learning
Plant diseases
Wheat
Yield failure

ABSTRACT

Context or problem: In recent decades, compounding weather extremes and plant diseases have increased wheat yield variability in France, the largest wheat producer in the European Union.
Objective or research question: How these extremes might affect future wheat production remains unclear.
Methods: Based on department level wheat yields, disease, and climate indices from 1980 to 2019 in France, we combined an existing disease model with machine learning algorithms to estimate future grain yields.
Results: This approach explains about 59% of historical yield variability. Projections from five CMIP6 climate models suggest that extreme low wheat yields, which used to occur once every 20 years, could occur every decade by the end of this century, but elevated CO_2 levels might lessen these events.
Conclusions: Heatwave-related yield losses are expected to double, while flooding-related yield losses will potentially decline by one third, depending on the representative concentration pathway. Ear blight disease is projected to contribute to 20% of the expected 400 kg ha^{-1} average yield losses by the end of the century, compared with 12% in the historical baseline period. These projections depend on the timing of anthesis, currently between late May and early June in most departments. Anthesis advancing to early May would shift losses primarily to heavy rainfall and low solar radiation.
Implications or significance: French wheat production must adapt to these emerging threats, such as heat stress, which until recently had little impact but may become the primary cause of future yield losses.

1. Introduction

In recent years, the world has witnessed increasing year-to-year variability in wheat yields due to compounding factors such as climate extremes and plant diseases (Bezner Kerr et al., 2022; Gaupp et al., 2020; Liu et al., 2021; Schauberger et al., 2018). These factors pose a significant challenge to global food security, as they can lead to more frequent and severe wheat yield downturns worldwide (Nóia Júnior et al., 2021; Trnka et al., 2014).

France, a major player in global wheat production, accounting for 10 % of the world's wheat exports (FAO stat, 2022), has also faced its share of challenges. Historical climate events, such as the prolonged heatwave in 2003 or the extremely wet and warm season of 2016, had caused significant wheat production losses (Baruth et al., 2022; Ciais et al., 2005; FAO stat, 2022; Nóia Júnior et al., 2023b).

Wheat yield variability in France is influenced by a multitude of factors, including droughts, heatwaves, heavy rainfall, flooding, low solar radiation, and plant diseases (van der Velde et al., 2020, 2012).

* Corresponding author.
E-mail address: senthold.asseng@tum.de (S. Asseng).

https://doi.org/10.1016/j.fcr.2024.109703
Received 30 January 2024; Received in revised form 25 November 2024; Accepted 4 December 2024
Available online 12 December 2024

These drivers impact wheat growth at various stages, but primarily during anthesis and grain development and filling. While previous studies have emphasized the significance of these factors, they are often not fully integrated into climate change-related wheat yield projections (Ben-Ari et al., 2018; Boote et al., 2013; Rötter et al., 2018).

While much research has focused on the impact of individual climatic drivers like heatwaves and droughts on wheat production at European scale or globally (Asseng et al., 2011; Battisti and Naylor, 2009; Lobell et al., 2011; Webber et al., 2020, 2018). The role of crop diseases in agricultural risk assessments has been comparatively overlooked. This gap in research can lead to overly optimistic predictions, as it often disregards the interactions between climate and disease risks (Nóia Júnior et al., 2023a; Raymond et al., 2020).

Recent extreme weather events in France, such as in 2016, underscore the importance of considering compound climate extremes and crop diseases in agricultural risk assessments. In that year, France faced an unprecedented sequence of events, including heavy rainfall, crop diseases, low solar radiation, and anoxia, resulting in a 25 % drop in national wheat yield compared to the previous five-year average and some departments within the breadbasket area experienced a dramatic 55 % decline in wheat yields (Ben-Ari et al., 2018; Nóia Júnior et al., 2023b). This extreme decline had severe economic consequences (Simoes, 2022), underscoring the need for a more comprehensive understanding of the factors driving wheat yield variability.

This study aims to quantify the causes of historical wheat yield failures in the breadbasket area of France, with a particular focus on the combine effects of plant diseases and abiotic stresses, and analyze how these drivers may impact future wheat production.

2. Material and methods

2.1. Sites, weather and wheat phenology and yield data

The breadbasket of France is a high wheat yielding area (average wheat yield of 7.4 t ha^{-1} from 2011 to 2020) with 2.8 million ha of wheat, which extends over the northern part of the country and accounts for around 70 % of France's total wheat production (Fig. 1a) (Ben-Ari et al., 2018). This area is characterized by a temperate climate without particularly dry and warm summers, classified as marine west coast climate type Cfb, according to Köppen-Geiger climatic zone (Peel et al., 2007).

We divided the breadbasket of France into five agroclimatic homogeneous areas based on year-to-year yield anomalies, following a methodology previously employed by Nóia Júnior et al. (2021) (Fig. 1a). Within each agroclimatic homogeneous area we chose specific weather stations to represent the region. Some areas required two weather stations, while others only needed one, in accordance with the distribution of research stations previously used by Nóia Júnior et al. (2023), which aimed to represent the key agricultural regions in France. Supplementary Table S1 provides the geographic coordinates for these weather stations. Long-term daily weather data (1980–2019) encompassing daily maximum and minimum temperatures, solar radiation, and rainfall were sourced from each weather station.

Wheat yield data from 1980 to 2019 at the departmental (Nomenclature of Territorial Units for Statistics [NUTS] level 3) spatial scale were collected from official survey data provided by the French Ministry of Agriculture (Agreste, 2022). Yields in the breadbasket were aggregated considering the harvested area of each agroclimatic homogeneous areas. All yield data were corrected at 15 % moisture content. This value may vary with cultivar, cropping season, or location. However, as specific moisture data for each case were unavailable, we adopted a fixed value of 15 %, which is commonly used for wheat harvests (Abdollahpour et al., 2020).

To calculate climate and disease indices during key phenological phases (see below), we simulated the dates of the growth stages GS31 (ear at 1 cm; Zadoks growth scale) and anthesis (GS61) at the location of the height weather stations for the period 1980–2019 using the crop growth model CHN for a single wheat cultivar (Laberdesque et al., 2017, Le Bris et al., 2016). The CHN is a process-based crop model developed by Arvalis that simulates the daily soil-plant-atmosphere flows of carbon (C), water (H), and nitrogen (N), hence the name CHN. It includes a complete wheat phenology sub-model. This model has demonstrated satisfactory accuracy in simulating wheat phenology within France's breadbasket area (Supplementary Figure S3). Hereafter the period of anthesis was defined as ± 15 days around GS61, and the grain filling period as the period between GS61 plus 45 days (assuming a grain filling period of 45 days). For the future, we assumed a range of fixed dates for anthesis and maturity to consider possible changes in these (see subsection 2.7). The overlap between anthesis (± 15 days around GS61) and grain filling (GS61 to GS61 +45 days) reflects the physiological processes influencing grain yield. The period primarily determining grain number setting begins before anthesis and extends slightly beyond GS61, while grain filling, which influences grain size, starts at GS61 and continues until physiological maturity (Calderini et al., 2021; Reynolds et al., 2022). This overlap captures the interactive phase where grain number and size are simultaneously set, recognizing that grain yield is

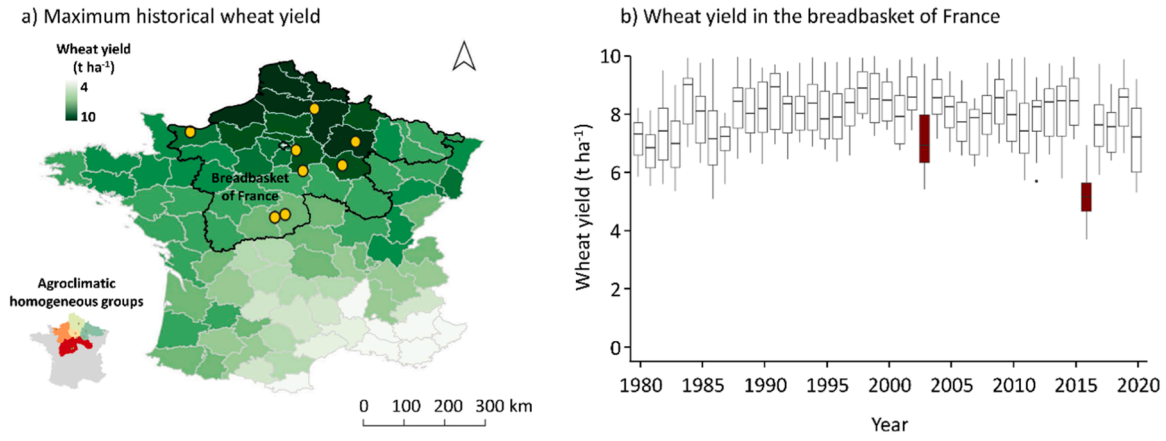

Fig. 1. Spatio-temporal pattern of trend-corrected wheat yield in the breadbasket of France. (a) Spatial distribution of the highest department level wheat yield observed from 1980 to 2019. The breadbasket area of France is delineated with a bold black contour line. Yellow dots indicate the eight locations studied. Inset map shows the agroclimatic homogeneous departments used for estimations of wheat yield losses. (b) Boxplot of the distribution of trend-corrected wheat yields in the breadbasket of France from 1980 to 2019. Low yielding anomalies in 2003 and 2016 are highlighted in dark red, which are in the 10th percentile of the historical observed wheat yield from 1980 to 2019.

the product of grain number per unit area and average grain size.

2.2. Extreme low yield and weather conditions analysis

To better understand the causes and spatial distribution of extreme declines in wheat yield during certain years, such as 2003 and 2016 (Fig. 1b), we analyzed the weather conditions in the wheat breadbasket during these low-yield seasons. This analysis, shown in results subsection 3.1, involved the assessment of long-term daily weather data (1980–2019) to calculate seasonal anomalies in maximum temperature and rainfall from May 1st to June 30th, a critical period encompassing wheat anthesis and grain filling. The data, with a global grid resolution of ½° x $^{5}/_{8}$°, was sourced from the Prediction Of Worldwide Energy Resources (NASA POWER) dataset (Team, 2021). Weather anomaly is calculated as the difference between the weather conditions of the analyzed year (2003 or 2016) and the long-term average spanning from 1980 to 2019.

In subsection 2.5, we detail the construction of our statistical models, which were developed using climatic indices as predictors for wheat yield anomalies. These indices were calculated based on data from the eight weather stations, covering a 40-year period, resulting in a dataset of 320 unique combinations of specific sites and individual years.

The climatic indices for these eight weather stations were correlated with yield anomalies (see subsection 2.3) at the departmental spatial scale from 1980 to 2019. This means that the climatic indices from each weather station were correlated with the wheat yield anomaly of the department to which the weather station belonged. In cases where an agroclimatic homogeneous area was represented by two weather stations in two different departments, estimates of yield anomaly and the causes of yield losses were calculated separately for each weather station, and the results were then averaged to represent the region.

2.3. Yield detrending and wheat yields relative anomaly

We removed long-term yield trends in each department independently, to remove possible effects of technological improvements throughout the studied period, as described in Guarin et al. (2020). To remove the long-term trend, we estimated a linear slope through the historical yield series from 1980 to 2019 to identify the average yield increase per year, as suggested by Ben-Ari et al. (2018). Yield of each year from 1980 to 2019 was adjusted to 2019 yield levels by adding the slope for each year difference from 1980 until 2019. Yield anomalies (Y_{anm}) at the department level were then computed as the percent difference between observed yields (Y_{obs}) and average yields (Y_{avg}, average of the trend-corrected yields) divided by Y_{avg}:

$$Y_{anm}(i,t) = \frac{Y_{obs}(i,t) - Y_{avg}(t)}{Y_{avg}(t)} \times 100 \quad (1)$$

where i indicates the department and t, the harvest calendar year.

2.4. Extreme climate and plant diseases indices

Indices that drive yield loss were identified from the literature (Ben-Ari et al., 2018; Nóia Júnior et al., 2023b; Nóia Júnior et al., 2023). We computed diseases indices for ear blight and foliar fungal and climate indices for heavy rainfall at anthesis and extreme drought, heat, flooding, and low solar radiation for the anthesis and grain filling periods. In total, we calculated 11 indices, being nine indices for weather and two for crop diseases, all used as predictors in the statistical models.

Thresholds were defined for each climate index based on probability distribution for the baseline period of 1980–2021, considering the height weather stations within the breadbasket area. For climate change assessment, a baseline of 1980–2021 was used, while model construction used 1980–2019 due to department-level yield data availability only up to 2019 at the time of model development. To compute drought and flooding indices, we calculated a water balance as the sum of daily rainfall (Rain) minus cumulative reference evapotranspiration (Eto, from Hargreaves and Samani 1985) during each period (anthesis and grain filling). Based on this water balance, we considered drought as the number of days during anthesis (GS61) and grain filling (from GS61 to grain maturity – fixed period of 45 days, GS61 + 45 days) with daily accumulated (Rain – ETo) < -168 mm (or 20th percentile), and flooding, as the number of days during anthesis and grain filling in which daily accumulated (ETo - Rain) > 30 mm (or 10th percentile). This is a method similar to the one used by Nóia Júnior et al. (2023b). Typically, plants require high soil water saturation to experience severe negative effects on yield (Liu et al., 2021), whereas even mild to moderate water deficits can impact yield. Taking this into account, we defined drought as the 20th percentile of daily accumulated (Rain – ETo), while flooding was determined as the 90th percentile of daily accumulated (Rain – ETo) (Alifu et al., 2022). We defined a heat index as the number of days with maximum temperature above 30 °C (90th percentile) (Nuttall et al., 2018), a low solar radiation index as the number of days with solar radiation below 7 MJ m^{-2} d^{-1} (1th percentile) (Nóia Júnior et al., 2023b), and an heavy rainfall index as the number of days with rainfall above 17 mm (99th percentile) (Seneviratne et al., 2021).

The ear blight model predicts disease incidence, while the fungal foliar disease model predicts disease severity. Both models are described below. Severity assesses damage and visible symptoms on individual plants, while incidence quantifies the proportion of affected plant or field areas. Severity measures impact, while incidence detects the presence of disease.

Ear blight or fusarium ear blight *(Fusarium graminearum, Fusarium culmorum),* usually infects wheat plants during anthesis under warm and humid conditions, and high rainfalls during anthesis. We computed an ear blight index based on the empirical model of Madgwick et al. (2011), which predicts the disease incidence, and is given by:

$$\text{Ear blight index} = 100 \frac{\exp(-15.3 + 0.941\ Tmean_{May} + 0.069\ Rainfall_{1week\,around\,anthesis})}{1 + \exp(-15.3 + 0.941\ Tmean_{May} + 0.069\ Rainfall_{1week\,around\,anthesis})} \quad (2)$$

where $Tmean_{May}$ (°C) is the mean temperature in May and $Rainfall_{1week\text{-}June}$ (mm) is the cumulative rainfall during the anthesis period.

The survival of fall infection of winter wheat by fungal foliar diseases such as Septoria blotch (*Zymoseptoria tritici*) is favored by warm temperatures during the winter (Ben-Ari et al., 2018; Chaloner et al., 2019; te Beest et al., 2009). The development of these foliar fungal diseases then depends on wet environments, especially on rain in March and April (El Jarroudi et al., 2016). As such, we computed a fungal foliar diseases index based on a model previously developed by te Beest et al. (2009), which predicts the disease severity and is given by:

$$\text{Fungal foliar index} = 0.046\ Rain_{(GS31-\ 140)\ \rightarrow\ (GS31-\ 30)} + 0.042\ Tmin_{(GS31-\ 140)\ \rightarrow\ (GS31-\ 30)} - 6.69 > 0 \quad (3)$$

where, $Rain_{(Gs31-\ 140)\ \rightarrow\ (Gs31-\ 30)}$ is the accumulated rainfall (mm) and $Tmin_{(Gs31-\ 140)\ \rightarrow\ (Gs31-\ 30)}$ is the mean daily minimum temperature (°C)

between 140 and 30 day of the year before GS31 (GS31 was simulated by CHN to quantify past wheat yield losses and kept fixed for assessing future yield losses).

2.5. Modeling yield anomalies with random forest machine learning

A statistical model was developed for yield anomalies using department level yield observations from 1980 to 2019, together with seasonal climate indices of drought, heat, flooding, and low solar indices calculated around anthesis and during grain filling, as well as heavy rainfall around anthesis and ear blight and foliar fungal diseases indices (as described in the subsection 2.4). Observed yield anomalies were multiplied by trend-corrected average yield from 1980 to 2019 and converted to trend-corrected yield (described in subsection 2.3), which was used to build the statistical model.

A random forest machine learning approach was applied to identify the best combination of explanatory variables using the function random Forest of the R package 'randomForest' (R Core Team, 2017). Random forest was set with 500 trees, with three variables tried at each split. The set up of Random Forest followed the sensitivity analyzes which indicated where the quality of the predictions plateaued (Supplementary Figure S2). To evaluate the predictive performance of the trend-corrected yield model (henceforth called yield model), a leave-one-out cross validation (LOOCV) was performed using the random forest with seven of the eight locations to select the best combination of inputs each year, and it was then tested on the excluded location (Sweet et al., 2023). This process was repeated for each location for a total of eight interactions. The relative root mean squared error of prediction (*rRMSEp*) (Wallach and Goffinet, 1987), the coefficient of determination (r^2) and the Nash-Sutcliffe model efficiency coefficient (NSE) (McCuen et al., 2006) were then calculated based on the estimated trend-corrected yield (henceforth called estimated yield) at the tested location together with the corresponding observed yield.

To account for the effects of increase in atmospheric CO_2 concentration in future climate scenarios (Supplementary Figure S13), we incorporated the CO_2 growth stimulus effect on simulated trend-corrected yield, as described in Tebaldi and Lobell (2018) (Supplementary Table S2). As the interaction of CO_2 with certain yield-reducing factors such as heat, flooding, and plant diseases remains uncertain, we did not account for these interactions when calculating future yield losses causes due to climate change.

2.6. Quantifying the impacts of individual yield limiting factors

To quantify the impacts of individual yield limiting factors, we used the random forest equation trained as described above. First the equation was applied using all climate and plant diseases indices to calculate yield in a target year in the period 1980–2019 (Supplementary Figure S1). The random forest equation was then applied again by modifying one explanatory variable (a climate or plant diseases index) value at a time by replacing the target year value with the corresponding value for each of 1980–2019 (Supplementary Figure S1). This step was repeated, replacing the value of each climatic or disease index in turn. Thus, the contribution of each yield limiting factor in each year of the period from 1980 to 2019 was calculated as the difference between the estimated trend-corrected yield from the models with all variables for a target year, and the estimates from the statistical models with all variables of the target year except one from the average of each year from 1980–2019 (excluding the target year), as schematically shown in the Supplementary Figure S1. This is similar to the method proposed by Asseng et al. (2011) and used by Nóia Júnior et al. (2023b) for separating the impacts of temperature from other factors on yield.

2.7. Climate change scenarios and extreme low yield definition

Daily weather data for the 1985–2100 period were drawn from the Inter-Sectoral Impacts Model Intercomparison Project (ISIMIP; (Lange, 2019)), which provides trend-preserving, bias-adjusted and spatially disaggregated climate model outputs from the Coupled Model Intercomparison Project phase 6 (CMIP6; (Eyring et al., 2016)). Before 2015, these are produced by climate models forced by historical trends of main natural and anthropogenic factors. After 2015, simulations follow the Shared Socioeconomic Pathway (SSP) and Representative Concentration Pathway (RCP) (O'Neill et al., 2016). In this study we considered the scenarios SSP1–2.6 and SSP5–8.5. The IPCC describe SSP1–2.6 as a "low" and SSP5–8.5 as a "very high" greenhouse gas emissions scenario (IPCC, 2021; O'Neill et al., 2020). We considered five CMIP6 models (GFDL-ESM4, IPSL-CM6A-LR, MPI-ESM1–2-HR, MRI-ESM2–0 and UKESM1–0-LL) that include high, medium and low climate sensitivity models similar to the full CMIP6 distribution (IPCC, 2021) (Jägermeyr et al., 2021), which we use to illustrate the bottom and upper tail of future risks. We used daily weather data from the ISIMIP (Heinicke et al., 2022) downscaled projections for the five selected models to quantify future frequency of drought, heat, flooding and low solar radiation occurrence both during anthesis (fixed on 1 June ± 15 days) and grain filling (from 1 June to 31 July), as well as heavy rainfall during anthesis. These indices together with the indices for ear blight and foliar fungal diseases previously described in subsection 2.1, allow us to estimate yield and its losses.

Current wheat cultivars are expected to have early anthesis and shorter grain filling period due to higher temperatures in future. Asseng et al. (2015) suggested a combination of delayed anthesis with increased grain filling rate as an adaptation for wheat to increased temperature. These traits could boost global wheat production by 7 % (Asseng et al., 2019). In consideration of the uncertainties surrounding phenology, such as potential shortening of phenological stages due to rising temperatures and consequent shifts in growing degree day accumulation, or the possibility of breeders developing cultivars with delayed anthesis and increased grain-filling rates to maintain current phenological timing, in our analysis, we considered a fixed future scenario where anthesis occurs on June 1st with grain filling from June 1st to July 31st (operating on the assumption of delayed anthesis matching current conditions in France). To reduce uncertainties regarding the fixed anthesis date, additional projection with anthesis fixed on 1st May ± 15 days and grain filling from 1 May to 15 June was performed.

Projections for extremely low yield frequency and future causes of yield losses are shown as 30 years running mean (*i.e.* value shown for 2015 is the average from 1986 to 2015, and for 2016 the average from 1987 to 2016). Extreme low yield for the breadbasket of France was estimated for each GCM separately and defined as below the 5th percentile (Nóia Júnior et al., 2021; Vogel et al., 2021) yield during 1850–2020, a period when all climate scenarios were similar.

3. Results

3.1. Extreme low yield and weather conditions in the breadbasket of France

In the breadbasket of France, winter wheat typically experiences a 10-month growing season, spanning from early October to late July. Anthesis is commonly observed from mid-May to early June (Supplementary Figure S3), while grain filling occurs during the months of June and early July. Taking this into account, we analyzed the spatial distribution of maximum temperatures, accumulated rainfall anomalies during anthesis-grain filling period (from May 1st to June 31st), as well as the yield anomalies for both the 2003 and 2016 cropping seasons in France (Fig. 2).

The average maximum temperature during May and June of 2003 was about 2°C higher than the historical period of 1980–2019 in the breadbasket of France. In the central part of France, located outside the breadbasket area, the maximum temperature was even higher—up to 5°C above the average (Fig. 2a). From May to June in 2003, there was

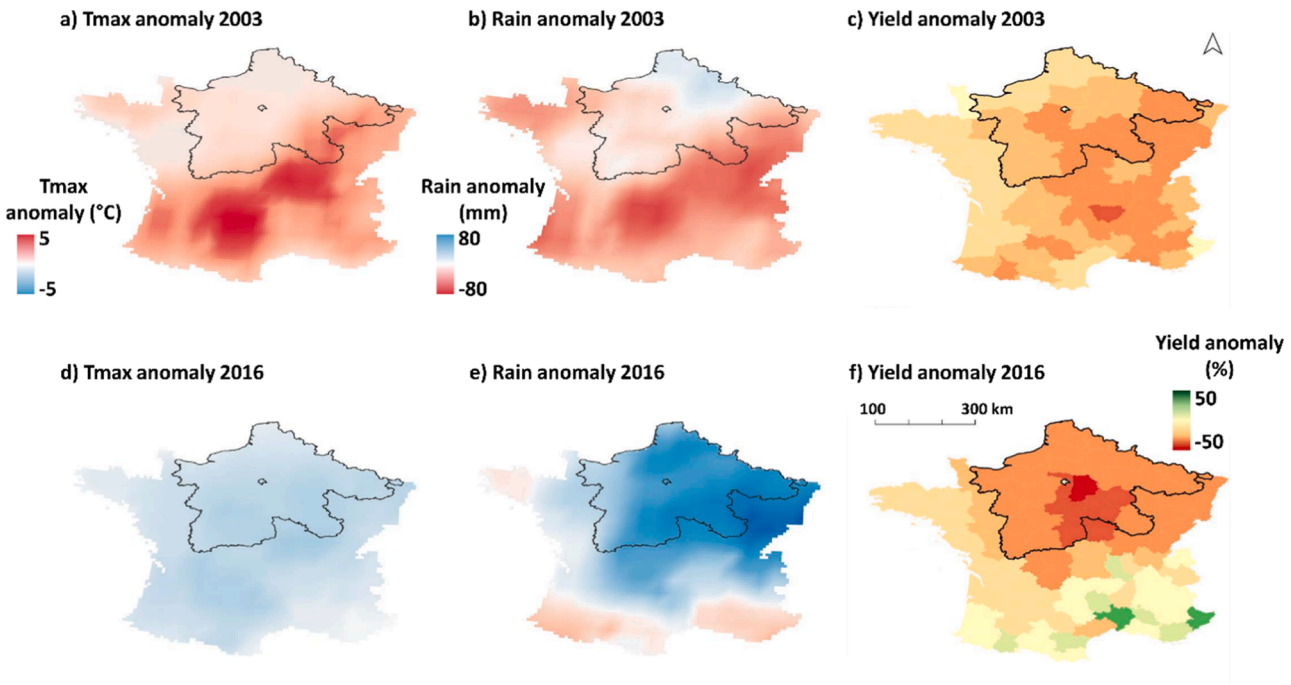

Fig. 2. Weather anomalies during two extreme low yielding wheat cropping seasons in France. Spatial pattern of the observed anomaly of (a, d) average maximum daily temperature and (b, e) accumulated rainfall during anthesis-grain filling (1st May to 31st June), and observed yield loss (c, f) for the 2003 and 2016 wheat harvest year. The breadbasket of France is delineated with a black contour line.

less rainfall than usual, up to 80 mm below average, in the central-eastern part of France (Fig. 2b). Within the breadbasket, rainfall during this period was near the average, with approximately 20 mm less in the southern breadbasket area and an increase of up to 10 mm in other parts compared to the historical average (1980–2019). This rainfall variation within the French breadbasket represents less than 10 % of the expected 120 mm of accumulated rainfall for the area between May and June. In 2003, wheat yield was mainly 5–10 % lower than expected within the breadbasket, while some areas in the northern part came close to the expected yield (Fig. 2c). The most significant decreases in yield were seen in areas located further south of France (outside the breadbasket), where higher temperatures and lower rainfall led to declines of up to 20 % compared to the historical average.

In 2016, the maximum temperature closely approached the average for the months of May and June, exhibiting a deviation of 0.5–1 °C lower than expected (Fig. 2d). Cumulative rainfall during the same period exceeded historical averages by up to 80 mm, signifying an elevation of 66 % (or two-thirds; Fig. 2e). In the central area of France's breadbasket, area with a significant surplus of rainfall in 2016 compared to historical average, yield exhibited a considerable decline of up to 50 % below the historical average (Fig. 2f). In contrast, in the south of France (outside the breadbasket), where the accumulated rainfall was slightly below historical averages, a modest surplus in yield was observed, with specific departments even attaining yields surpassing the historical average by as much as 20 %.

3.2. Modeling yield in the breadbasket of France

During the training phase, we achieved satisfactory results with a r^2 of 0.98 and a RMSE of 0.09 t ha^{-1}, indicating an error of around 1 % (Fig. 3). Additionally, the NSE was calculated to be 0.97. The cross-validation of the model gave an rRMSEp equals 0.48 t ha^{-1}, corresponding to a 5 % error. The r^2 was 0.59, while NSE remained at 0.48. This cross-validation exercise underscored the model's commendable precision ($r^2 > 0.6$), efficiency (NSE > 0), and low average error (rRMSEp < 5 %). Notably, the model effectively captured the remarkably low yield experienced in 2016.

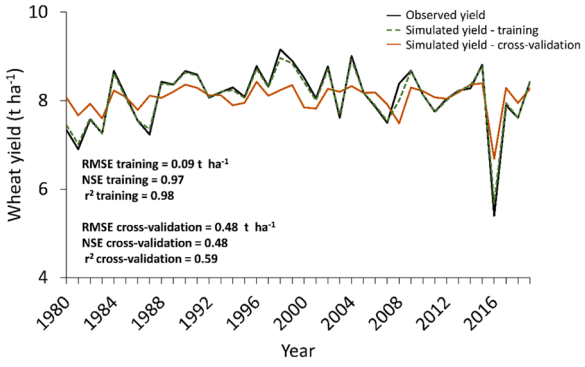

Fig. 3. Estimated and observed trend corrected wheat yields in the breadbasket of France. Year-to-year variability from 1980 to 2019 of observed (black solid lines) and simulated yield during the training (green dashed lines) and cross-validation (orange line) of the random forest machine learning approach for wheat trend corrected yield. Estimated results are from a leave-on-out cross validation, leaving all years from a location out of the training set with a random forest machine learning approach. The root mean squared error (RMSE), coefficient of determination (r^2) and Nash-Sutcliffe modeling efficiency (NSE) are shown.

3.3. Quantified causes of yield losses

Building upon the capabilities of the random-forest machine learning model in evaluating yield and anomalies, our study undertook a comprehensive analysis of the factors contributing to yield losses within the breadbasket area over the period 1980–2019 (Fig. 4). Our findings elucidate that the notable drop in wheat yield during the 2016 cropping season stems from the combination of distinct factors. This encompasses flooding incidences during grain filling, as well as low solar radiation during anthesis, culminating together in an estimated 80 % reduction in wheat yield (Supplementary Figure S12). Adding to this effect, heavy

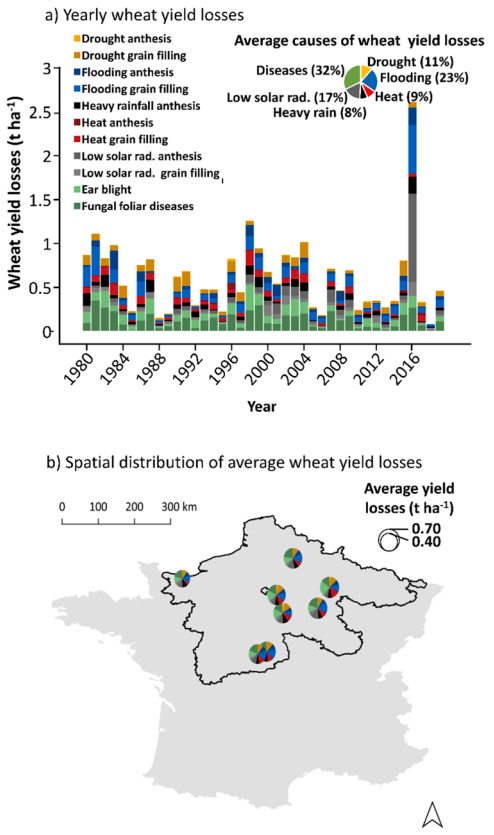

Fig. 4. Breakdown of causes of wheat yield losses in France's breadbasket. (a) Year-to-year yield losses causes and (b) spatial distribution of average yield losses in France's breadbasket. The yield losses are relative to the average of estimated trend-corrected yield for 40 cropping seasons from 1980 to 2019 in the breadbasket of France. In (b) the estimations are shown for the locations of Égreville, Chevry-Cossigny, Saint-Quentin, Saint-Florent-sur-Cher, Fagnières, Issodun, Barbarey-Saint-Sulpice, and Rots.

rainfall during anthesis results in an extra 15 % decrease. Also, ear blight contributes to a 7 % reduction, while fungal foliar diseases lead to a 2 % reduction. Together, these factors significantly contribute to the decline in wheat yield in 2016. Our analysis of the 2003 wheat yield reduction indicates that heat, drought, and plant diseases collectively caused a two-thirds decline in yields.

On average, our results indicate that 32 % of yield losses in France can be attributed to plant diseases (19 % Fungal foliar disease and 13 % Ear blight), with an additional 23 % attributed to flooding, 17 % to constrained solar radiation, 11 % to drought, and 8 % to intense rainfall events. Notably, these proportions exhibit nuanced variations across distinct sub-department within the encompassing span of France's breadbasket (Fig. 4b).

3.4. Future frequency of extremely low yield years

The future frequency of extremely low yield years shows evidence of a trend towards a subtle increase. This trend involves moving from a current 5 % frequency to around 9 % by the end of the century (Fig. 5a), regardless of the climatic scenario (SSP5 2.6 or SSP5 8.5), and without considering the potentially positive impacts of CO_2.

When we take into account the potential influence of CO_2 (Fig. 5b), which could result in increased crop growth (Tebaldi and Lobell, 2018) (Supplementary Figure S5), the results show a steep decrease in the occurrence of extremely low yield events in the future. This suggests that these events could cease to exist by the end of the century, regardless of the climate scenario.

These results are calculated considering a fixed anthesis on 1st June, which is currently the case. However, a similar frequency of extreme low yield years is expected to occur if the anthesis date is brought forward to May 1st (Supplementary Figure S8).

3.5. Future causes of yield losses in France's breadbasket

Because of our current lack of knowledge on the interactions of CO_2 with the yield reducing factors considered in this study (see the Discussion section), we did not consider the effect of CO_2 on yield loss causing factors. The factors contributing to yield losses in France's breadbasket are expected to change by 2100 (Fig. 6). In the SSP5–2.6 climate scenario, the projected causes of yield losses show fluctuations from 2015 to 2100 (Fig. 6a). Heat and ear blight are projected to increase significantly, causing losses of up to 70 kg ha^{-1} $year^{-1}$ by the end of the century. This is a 40 % compared to the current 50 kg ha^{-1} per year losses due to heat and ear blight. Heavy rainfall is projected to cause a slight increase in yield loss, rising from the current average of 5.5 t ha^{-1} $year^{-1}$ to 7 t ha^{-1} $year^{-1}$. The negative impact on yield of low solar radiation and fungal foliar diseases are projected to decrease by the end of the century. Projected yield losses from flooding and drought under the SSP5–2.6 climate scenario show no discernible trend (Supplementary Figure S6).

In the SSP5–8.5 climate scenario, there are more noticeable shifts in

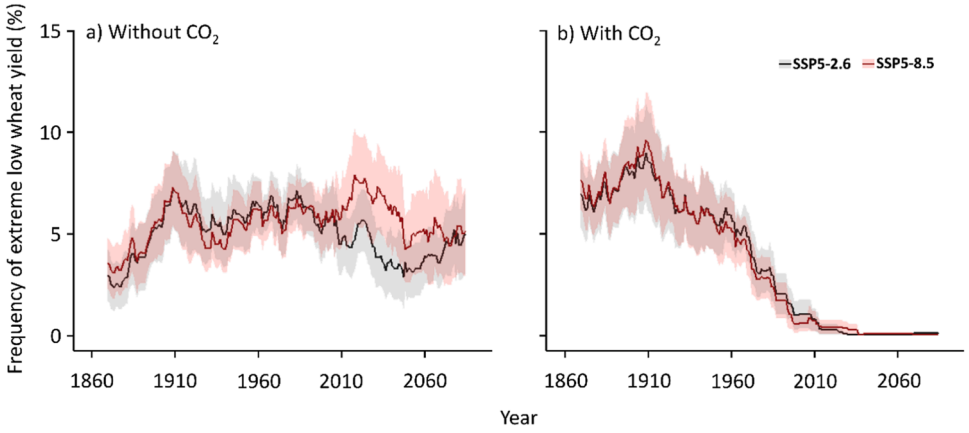

Fig. 5. Projected frequency of extreme low wheat yield years in the breadbasket of France. Estimated 30 years running mean frequency of extreme low production under SSP5–2.6 (black trace) and SSP5–8.5 (red trace) from 1865 to 2085 for the breadbasket of France. The projections are shown (a) to indicate the impact of elevated CO_2 on yield shown without elevated CO_2 and (b) with the effects of elevated CO_2. Lines are ensemble means based on five CMIP6 GCMs (lines) and shading shows ± 1 s.e. These projections consider a fixed anthesis on 1 June.

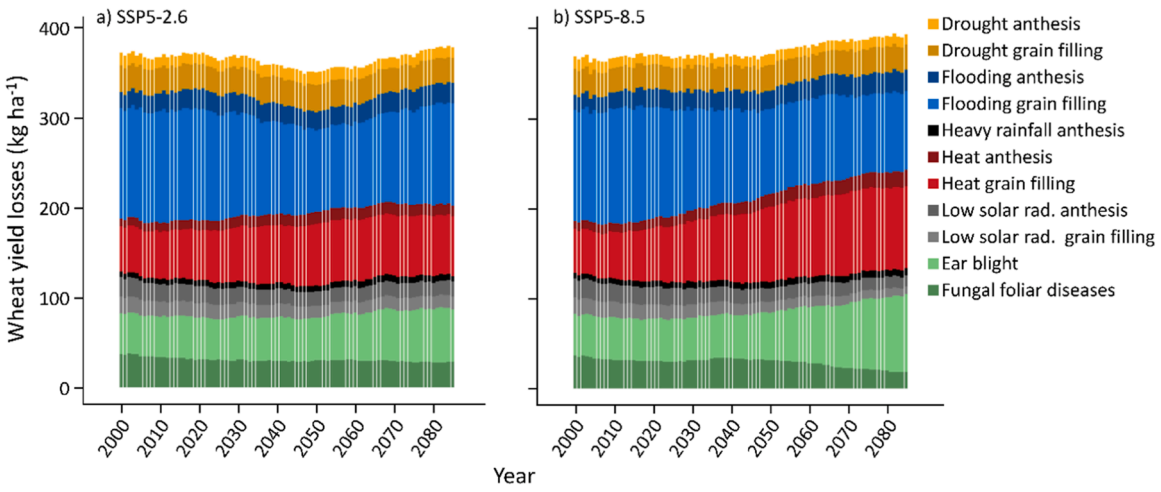

Fig. 6. Future causes of wheat yield losses in France's breadbasket. Thirty-years running mean of the causes of yield losses in France's breadbasket between 2015 and 2100. Bars are ensemble means based on five bias-adjusted CMIP6 global climate models (GCMs) for (a) SSP5–2.6 and (b) SSP5–8.5, with a fixed anthesis on 1 June and grain filling from 1 June and 15 July. Climate projections for monthly maximum and minimum temperature, solar radiation, and rainfall at Égreville are shown in Supplementary Fig. S4. The projected yield losses are relative to the average of estimated trend-corrected yield from 1980–2019 in France's breadbasket.

the causes of yield losses (Fig. 6b). The losses caused by flooding during grain filling are projected to decrease by the end of the century. Currently leading to an average loss of about 120 kg ha^{-1} year^{-1}, this could drop to 90 kg ha-^{1} year^{-1} by the end of the century. Under the SSP5–8.5 climate scenario, yield losses due to heat are projected to almost double by the end of the century (Supplementary Figure S7). The average yield losses from heat during grain filling could increase from 50 kg ha^{-1} year^{-1} in the period 1098–2019–90 kg ha^{-1} year^{-1} by 2100. As heat increases, ear blight is projected become a major cause of yield losses in French's breadbasket, contributing to around 20 % of total yield losses by 2100 (Fig. 6). By the end of the century, yield losses due to low solar radiation and fungal foliar diseases are projected to be half of current levels. On the other hand, projected yield losses due to drought during anthesis show varied fluctuations without a clear pattern between 2015 and 2100 (Fig. 6 and Supplementary Figure S6-S7).

To enhance the robustness of our analysis, we applied the same methodology to quantify yield losses in the future under the influence of climate change, assuming an earlier anthesis onset in the beginning of May. In this scenario, we project that due to the reduced solar radiation during this period and an increased number of heavy rainfall events, these factors would lead to the most significant productivity losses. If this were to occur, we project even greater magnitudes of productivity loss assuming anthesis is brought forward one month in the future (Supplementary Figure S9-S11).

4. Discussion

To separate the historical and future impact of single climatic events on wheat yield in France's breadbasket, we combined department level yields, calculated disease damage and climate indices with a machine learning algorithm for estimating grain yield losses. Our model presents similar performance (*rRMSEp* of 5 % from LOOCV one location out or 8 % from LOOCV one year out; Supplementary Table S3) in estimating yield in France compared to other recent studies (*rRMSEp* varying from 10 % to 18 % (Paudel et al., 2022)). Our results showcase the random forest method's ability to quantify factors influencing yield losses (Fig. 4). This approach is consistent with earlier research that assessed the impacts of different variables on yield using linear models (Nóia Júnior et al., 2023b), which found a similar quantification of the causes of yield loss in the breadbasket of France in 2016. While our model yielded results comparable to those in the literature, further improvement could be achieved with an expanded training dataset, additional locations, or an ensemble of machine learning methods, as suggested in previous research (von Bloh et al., 2023).

Projections with five CMIP6 climate models under low (SSP5–2.6) and very high emissions (SSP5–8.5) scenarios suggest that current extreme low yields historically occurring once every 20 years, could become twice as frequent by the end of the century. Elevated atmospheric CO_2 concentration may help reduce the occurrence of such events (Fig. 5b). Some studies, such as Schauberger et al. (2021) and Liu et al. (2019), have found no historical or future evidence of increased wheat yield volatility across most of France, except for a few areas like the northwest, as highlighted by Pequeno et al. (2021), who also considered the potential benefits of CO_2. However, even with atmospheric CO_2 exceeding 400 ppm, extreme climate events in France can still lead to significant yield losses, with some departments experiencing yield reductions of over 50 % in certain years, as observed in 2016 (Nóia Júnior et al., 2023b). Our findings suggest that after the mid-2000s, extreme events due to CO_2 levels exceeding 400 ppm are projected to decrease, approaching zero by 2050. (Fig. 5b). However, it's important to acknowledge that the simplicity of accounting for CO_2 effects, both in our study and others (Tebaldi and Lobell, 2018), may not fully capture the complex interactions between CO_2 and other factors, such as flooding (Nóia Júnior et al., 2023a), which are not yet well understood.

Climate change results from rising atmospheric CO_2 levels, which elevate global average temperatures (IPCC, 2021). Numerous studies demonstrate the significant positive impact of elevated CO_2 on C3 crop yield. For example, with ample water and nutrient, it has been shown that wheat yields increase can reach about 19 % with elevated CO_2 in FACE experiments (from a CO_2 mixing ratio of 353–550 ppm) (Kimball, 2016). The same experiments showed that due to low stomatal conductance, transpiration decreases by 15 % and canopy temperature increased by 0.6 °C (Kimball, 2016). Decreased transpiration conserves soil moisture, potentially mitigating the impacts of drought, although increased canopy temperature may exacerbate heat stress. Further research is needed to understand how elevated CO_2 interacts with stressors such as heat and other factors, including plant diseases, flooding, heavy rainfall, and low solar radiation (Toreti et al., 2020). A unique study in a controlled environment indicated that high CO_2 may further increase the impacts of ear blight and Septoria blotch on wheat (Váry et al., 2015), but the implications of this study in the field are still unclear. Although the average yields may increase in the future with elevated CO_2 provided that nitrogen and water availability are adequate (Webber et al., 2018), there are uncertainties about the interactions with yield reducing factors under extreme weather conditions. Due to these uncertainties, we did not consider the potential impacts of elevated CO_2

when quantifying past and future causes of yield losses, as shown in Fig. 6.

Wheat production in France can be affected by excess water, causing flooding, reduced solar radiation and plant diseases. Our results show that these factors historically caused more yield losses than droughts and high temperatures (Fig. 2), as occurred in the 2016 cropping season (Ben-Ari et al., 2018; Nóia Júnior et al., 2023b; van der Velde et al., 2020). Excessive precipitation was found to be the main factor influencing wheat yields in France since the first half of the 20th Century (Ceglar et al., 2020), and drained areas account for 9 % of all arable soils in France (Jeantet et al., 2021). However, due to the recent increased heat and drought events in spring and summer (as in 2003, 2007, 2011, 2020 and 2022), excess rainfall has already shown a lower correlation with wheat yield in the last two decades, compared to previous periods (Ceglar et al., 2020). Our study suggests that, as a result of these changes, by the end of the century, there might be less yield loss from floodings occurring during grain filling. We emphasize that the water balance used here does not consider possible accumulations of water on the soil surface after heavy rains (due to the speed of infiltration of water into the soil, sometimes being lower than the intensity of the rain). This adds uncertainties to our projections. Despite this, we indicated that yield losses due to heavy rainfall during anthesis may increase by the end of the century (Supplementary Figure S7-S8), if higher temperatures accelerate phenology, causing anthesis to occur in early May (Supplementary Figure S10-S11). Heavy rainfall is also expected to become more frequent during other seasons and phenological stages throughout the year (Fischer and Knutti, 2015).

Heat and ear blight may become increasingly damaging to wheat yield in France's breadbasket (Fig. 6). This is mostly due to the projected future increase of up to 3°C in maximum monthly mean temperature combined with a decrease in monthly precipitation during grain filling (Supplementary Figure S4), further increasing heat stress. These results are in agreement with previous climate change impact studies, which have largely focused on heat, with national wheat yield losses of −4.6 % (varying from −4.2–5.2 %) in France when not considering increased atmospheric CO_2 (Zhao et al., 2017). In addition, winter and spring are expected to become warmer and wetter by the end of the century in the breadbasket of France (Supplementary Figure S4) (Ben-Ari et al., 2018; Ranasinghe et al., 2021), which contributes to ear blight infection spread (Madgwick et al., 2011; West et al., 2012; Xu, 2003). Ear blight is related to rainfall during anthesis and temperature during the preceding weeks (Madgwick et al., 2011). We project that ear blight will cause twice as much yield losses than currently (Fig. 6), but this is contingent on the anthesis date not advancing to mid-May. (Supplementary Figure S10-S11). The incidence of ear blight on wheat yield is also projected to double by 2050 in southern England, an area with similar edaphoclimatic conditions to the breadbasket in France (Madgwick et al., 2011). Yet, the ear blight model used here does not consider the initial inoculum but correlates it to higher spring temperatures as factors contributing to its rise. Although the initial inoculum benefits from high temperatures (Madgwick et al., 2011), factors such as the pre-crop in rotation with wheat (which also affects the initial inoculum) are neglected by the disease model, which adds uncertainty to the projections and could cause an overestimate of the disease's impact in some years. Estimated ear blight impacts on wheat yield are probably higher than foliar fungal diseases because of its less efficient control (Zhang et al., 2020).

Due to projected warmer and drier summers, studies suggest that Europe could experience summer droughts 11–28 times more frequently than it does now (Grillakis, 2019). Nonetheless, our results indicate that in France's breadbasket droughts during anthesis and grain filling may vary widely throughout the century but do not show a clear trend of increasing or decreasing frequency. The average amount of solar radiation reaching wheat canopies in France will increase (Supplementary Figure S4). Yet, it is expected that increased heavy rainfall will lead to more future wheat yield losses (Supplementary Figure S6-S7), while the influence of low solar radiation on yield is expected to diminish. (Supplementary Figure S6-S7). Here, we define a low solar radiation index as the number of days with solar radiation below 7 MJ m^{-2} d^{-1} during anthesis and grain filling, which is less than a third of the radiation usually received from May to July (Artru et al., 2018; Asseng et al., 2017). Chances of heavy rainfall occurrence in France may increase by 50–80 % if global average temperatures reach 3°C above pre-industrial conditions (Fischer and Knutti, 2015).

Our study is distinctive in its approach, isolating the effects of individual climate and disease-based factors on yield losses. Recognizing that different factors may necessitate distinct adaptation strategies, our results suggest that while the overall yield in France may increase due to elevated CO_2 levels, it may also face a heightened risk of encountering more frequent heat stress, a factor less prevalent in the past. Additionally, our findings underscore the growing importance of understanding and mitigating the increasing pressure from ear blight disease. This highlights the need for enhanced wheat breeding programs to develop new cultivars that are more resilient to heat and resistant to plant diseases. The management of extreme wheat losses in France holds significance not only for the country but also for other nations with similar climate conditions and that rely on French wheat exports. For instance, Algeria, a primary importer of French wheat, turned to increased wheat purchases from Russia in response to excessive rainfall affecting the quality of French wheat in 2021 (Muftuoglu, 2021).

While our model demonstrates a robust capability in quantifying yield losses and identifying key stressors, some limitations and uncertainties should be noted. Although the model integrates multiple climate and disease factors, it does not account for potential shifts in wheat phenology under future climate conditions, such as changes in the timing of anthesis and grain filling (Rezaei et al., 2018). Additionally, the historical data used to calibrate the model may limit its applicability in capturing extreme and unprecedented conditions anticipated in future climates (Nóia Júnior et al., 2023b). For instance, yield response data under prolonged and simultaneous exposure to multiple stressors (e.g., combined heat and drought stress) remain limited, potentially reducing the model's accuracy in such scenarios. Furthermore, our assumptions about CO_2 effects are based on simplified growth responses, without fully considering interactions with other yield-reducing factors such as heat, flooding, or plant diseases, which are complex and not yet fully understood. Future work should explore a more nuanced approach to CO_2 interactions and incorporate adaptive phenological responses to improve projections of climate impact on wheat yield.

In conclusion, our research highlights climate change's intricate effects on French wheat production. Addressing these multifaceted challenges demands a holistic approach, encompassing adaptation strategies and investigations into CO_2 interactions with environmental stressors. These efforts will be vital for wheat production resilience in a changing climate.

5. Conclusions

This study reveals the complex impacts of climate change on wheat yields in France's breadbasket. Using historical yield data, disease and climate indices with a random forest machine learning model, we identified heat stress, flooding, reduced solar radiation, and ear blight as the main contributors to yield losses over the past 40 years (1980–2019). Projections suggest that extreme low-yield events, historically occurring once every 20 years, could become twice as frequent by the end of the century under both low and high emissions scenarios. Elevated atmospheric CO_2 may reduce the occurrence of such events by enhancing yields, but uncertainties remain regarding its interactions with stressors like heat and disease. Our findings highlight the need for breeding programs to develop new wheat varieties with increased resilience to heat and disease pressures. Such efforts are crucial for maintaining wheat production stability in France and other regions with similar climatic conditions amid a changing climate.

CRediT authorship contribution statement

Rogério de S. Nóia Júnior: Writing – original draft, Visualization, Methodology, Formal analysis, Data curation, Conceptualization. **Pierre Martre:** Writing – review & editing, Supervision, Methodology, Conceptualization. **Senthold Asseng:** Writing – review & editing, Validation, Supervision, Resources, Methodology, Investigation, Conceptualization. **Marijn Van der Velde:** Writing – review & editing, Methodology, Conceptualization. **Heidi Webber:** Writing – review & editing, Methodology, Conceptualization. **Jean-Charles Deswarte:** Writing – review & editing, Supervision, Methodology, Conceptualization. **Jean-Pierre Cohan:** Writing – review & editing, Supervision, Methodology, Conceptualization. **Tamara Ben-Ari:** Writing – review & editing, Visualization, Methodology, Conceptualization. **Frank Ewert:** Writing – review & editing, Methodology, Conceptualization. **Alex C. Ruane:** Writing – review & editing, Methodology, Conceptualization.

Declaration of Competing Interest

The authors declare that they have no known competing financial interests or personal relationships that could have appeared to influence the work reported in this paper.

Acknowledgements

R.S.N.J. acknowledges support from ARVALIS and the Prince of Albert II of Monaco foundation through the IPCC Scholarship Program. The contents of this manuscript are solely the liability of R.S.N.J. and under no circumstances may be considered as a reflection of the position of the Prince Albert II of Monaco Foundation and/or the IPCC. P.M. acknowledges support from the Agriculture and Forestry in the Face of Climate Change: Adaptation and Mitigation (CLIMAE) Meta-program and AgroEcosystem division of the French National Research Institute for Agriculture, Food and Environment (INRAE). Support for A.C.R. was provided by the NASA Earth Sciences Directorate support of the GISS Climate Impacts Group and the Agricultural Model Intercomparison and Improvement Project (AgMIP). F.E. acknowledges support from the Deutsche Forschungsgemeinschaft (DFG, German Research Foundation) under Germany's Excellence Strategy – EXC 2070 – 390732324 (PhenoRob).

Appendix A. Supporting information

Supplementary data associated with this article can be found in the online version at doi:10.1016/j.fcr.2024.109703.

Data availability

Data will be made available on request.

References

Abdollahpour, S., Kosari-Moghaddam, A., Bannayan, M., 2020. Prediction of wheat moisture content at harvest time through ANN and SVR modeling techniques. Inf. Process. Agric. 7, 500–510. https://doi.org/10.1016/j.inpa.2020.01.003.

Agreste, 2022. Ministere de l'agriculture de l'agroalimentaire et de la foret. https://stats.agriculture.gouv.fr/disar/ (accessed 6.6.22).

Alifu, H., Hirabayashi, Y., Imada, Y., Shiogama, H., 2022. Enhancement of river flooding due to global warming. Sci. Rep. 12, 20687. https://doi.org/10.1038/s41598-022-25182-6.

Artru, S., Dumont, B., Ruget, F., Launay, M., Ripoche, D., Lassois, L., Garré, S., 2018. How does STICS crop model simulate crop growth and productivity under shade conditions? Field Crops Res. 215, 83–93. https://doi.org/10.1016/j.fcr.2017.10.005.

Asseng, S., Ewert, F., Martre, P., Rötter, R.P., Lobell, D.B., Cammarano, D., Kimball, B.A., Ottman, M.J., Wall, G.W., White, J.W., Reynolds, M.P., Alderman, P.D., Prasad, P.V. V., Aggarwal, P.K., Anothai, J., Basso, B., Biernath, C., Challinor, A.J., De Sanctis, G., Doltra, J., Fereres, E., Garcia-Vila, M., Gayler, S., Hoogenboom, G., Hunt, L.A., Izaurralde, R.C., Jabloun, M., Jones, C.D., Kersebaum, K.C., Koehler, A.-K., Müller, C., Naresh Kumar, S., Nendel, C., O'Leary, G., Olesen, J.E., Palosuo, T., Priesack, E., Eyshi Rezaei, E., Ruane, A.C., Semenov, M.A., Shcherbak, I., Stöckle, C., Stratonovitch, P., Streck, T., Supit, I., Tao, F., Thorburn, P.J., Waha, K., Wang, E., Wallach, D., Wolf, J., Zhao, Z., Zhu, Y., 2015. Rising temperatures reduce global wheat production. Nat. Clim. Change 5, 143–147. https://doi.org/10.1038/nclimate2470.

Asseng, S., Foster, I., Turner, N.C., 2011. The impact of temperature variability on wheat yields. Glob. Chang Biol. 17, 997–1012. https://doi.org/10.1111/j.1365-2486.2010.02262.x.

Asseng, S., Kassie, B.T., Labra, M.H., Amador, C., Calderini, D.F., 2017. Simulating the impact of source-sink manipulations in wheat. Field Crops Res. 202, 47–56. https://doi.org/10.1016/j.fcr.2016.04.031.

Asseng, S., Martre, P., Maiorano, A., Rötter, R.P., O'Leary, G.J., Fitzgerald, G.J., Girousse, C., Motzo, R., Giunta, F., Babar, M.A., Reynolds, M.P., Kheir, A.M.S., Thorburn, P.J., Waha, K., Ruane, A.C., Aggarwal, P.K., Ahmed, M., Balkovič, J., Basso, B., Biernath, C., Bindi, M., Cammarano, D., Challinor, A.J., De Sanctis, G., Dumont, B., Eyshi Rezaei, E., Fereres, E., Ferrise, R., Garcia-Vila, M., Gayler, S., Gao, Y., Horan, H., Hoogenboom, G., Izaurralde, R.C., Jabloun, M., Jones, C.D., Kassie, B.T., Kersebaum, K.-C., Klein, C., Koehler, A.-K., Liu, B., Minoli, S., Montesino San Martin, M., Müller, C., Naresh Kumar, S., Nendel, C., Olesen, J.E., Palosuo, T., Porter, J.R., Priesack, E., Ripoche, D., Semenov, M.A., Stöckle, C., Stratonovitch, P., Streck, T., Supit, I., Tao, F., Van der Velde, M., Wallach, D., Wang, E., Webber, H., Wolf, J., Xiao, L., Zhang, Z., Zhao, Z., Zhu, Y., Ewert, F., 2019. Climate change impact and adaptation for wheat protein. Glob. Change Biol. 25, 155–173. https://doi.org/10.1111/gcb.14481.

Baruth, B., Bassu, S., Ben Aoun, W., Biavetti, I., Bratu, M., Cerrani, I., Chemin, Y., Claverie, M., P, D.P., D, F., G, M., J, M., L, N.S., L, P., G, R., L, S., E, T., M, V.D.B., Z, Z., A, Z., M, V.D.B., S, N., 2022. JRC MARS Bulletin - Crop monitoring in Europe - July 2022 - Vol. 30 No 7. Publications Office of the European Union, Luxembourg (Luxembourg). https://doi.org/10.2760/577529 (online).

Battisti, DavidS., Naylor, R.L., 2009. Historical warnings of future food insecurity with unprecedented seasonal heat. Science 323 (1979), 240–244. https://doi.org/10.1126/science.1164363.

Ben-Ari, T., Boé, J., Ciais, P., Lecerf, R., Van der Velde, M., Makowski, D., 2018. Causes and implications of the unforeseen 2016 extreme yield loss in the breadbasket of France. Nat. Commun. 9, 1627. https://doi.org/10.1038/s41467-018-04087-x.

Bezner Kerr, R., Naess, L.O., Allen-O'Neil, B., Totin, E., Nyantakyi-Frimpong, H., Risvoll, C., Rivera Ferre, M.G., López-i-Gelats, F., Eriksen, S., 2022. Interplays between changing biophysical and social dynamics under climate change: implications for limits to sustainable adaptation in food systems. Glob. Chang Biol. 28, 3580–3604. https://doi.org/10.1111/gcb.16124.

Boote, K.J., Jones, J.W., White, J.W., Asseng, S., Lizaso, J., 2013. Putting mechanisms into crop production models. Plant Cell Environ. 36, 1658–1672. https://doi.org/10.1111/pce.12119.

Calderini, D.F., Castillo, F.M., Arenas-M, A., Molero, G., Reynolds, M.P., Craze, M., Bowden, S., Milner, M.J., Wallington, E.J., Dowle, A., Gomez, L.D., McQueen-Mason, S.J., 2021. Overcoming the trade-off between grain weight and number in wheat by the ectopic expression of expansin in developing seeds leads to increased yield potential. N. Phytol. 230, 629–640. https://doi.org/10.1111/nph.17048.

Ceglar, A., Zampieri, M., Gonzalez-Reviriego, N., Ciais, P., Schauberger, B., Van der Velde, M., 2020. Time-varying impact of climate on maize and wheat yields in France since 1900. Environ. Res. Lett. 15, 094039. https://doi.org/10.1088/1748-9326/aba1be.

Chaloner, T.M., Fones, H.N., Varma, V., Bebber, D.P., Gurr, S.J., 2019. A new mechanistic model of weather-dependent Septoria tritici blotch disease risk. Philos. Trans. R. Soc. B Biol. Sci. 374, 20180266. https://doi.org/10.1098/rstb.2018.0266.

Ciais, Ph, Reichstein, M., Viovy, N., Granier, A., Ogée, J., Allard, V., Aubinet, M., Buchmann, N., Bernhofer, Chr, Carrara, A., Chevallier, F., De Noblet, N., Friend, A. D., Friedlingstein, P., Grünwald, T., Heinesch, B., Keronen, P., Knohl, A., Krinner, G., Loustau, D., Manca, G., Matteucci, G., Miglietta, F., Ourcival, J.M., Papale, D., Pilegaard, K., Rambal, S., Seufert, G., Soussana, J.F., Sanz, M.J., Schulze, E.D., Vesala, T., Valentini, R., 2005. Europe-wide reduction in primary productivity caused by the heat and drought in 2003. Nature 437, 529–533. https://doi.org/10.1038/nature03972.

R. Core Team, 2017. R: A Language and Environment for Statistical Computing. R Foundation for Statistical Computing, Vienna, Austria. https://doi.org/http://www.R-project.org/.

El Jarroudi, Moussa, Kouadio, L., Bock, C.H., El Jarroudi, Mustapha, Junk, J., Pasquali, M., Maraite, H., Delfosse, P., 2016. A threshold-based weather model for predicting stripe rust infection in winter wheat. Plant Dis. 101, 693–703. https://doi.org/10.1094/PDIS-12-16-1766-RE.

Eyring, V., Bony, S., Meehl, G.A., Senior, C.A., Stevens, B., Stouffer, R.J., Taylor, K.E., 2016. Overview of the coupled model intercomparison project phase 6 (CMIP6) experimental design and organization. Geosci. Model Dev. 9, 1937–1958. https://doi.org/10.5194/gmd-9-1937-2016.

FAO stat, 2022. FAOSTAT: FAO statistical databases [WWW Document]. URL http://www.fao.org/faostat/en/#home (accessed 6.6.22).

Fischer, E.M., Knutti, R., 2015. Anthropogenic contribution to global occurrence of heavy-precipitation and high-temperature extremes. Nat. Clim. Change 5, 560–564. https://doi.org/10.1038/nclimate2617.

Gaupp, F., Hall, J., Hochrainer-Stigler, S., Dadson, S., 2020. Changing risks of simultaneous global breadbasket failure. Nat. Clim. Change 10, 54–57. https://doi.org/10.1038/s41558-019-0600-z.

Grillakis, M.G., 2019. Increase in severe and extreme soil moisture droughts for Europe under climate change. Science of The Total Environment 660, 1245–1255. https://doi.org/10.1016/j.scitotenv.2019.01.001.

Guarin, J.R., Asseng, S., Martre, P., Bliznyuk, N., 2020. Testing a crop model with extreme low yields from historical district records. Field Crops Res. 249, 107269. https://doi.org/10.1016/j.fcr.2018.03.006.

Hargreaves, G.H., Samani, Z.A., 1985. Reference crop evapotranspiration from temperature. Appl. Eng. Agric. 1, 96–99. https://doi.org/10.13031/2013.26773.

Heinicke, S., Frieler, K., Jägermeyr, J., Mengel, M., 2022. Global gridded crop models underestimate yield responses to droughts and heatwaves. Environ. Res. Lett.

IPCC, 2021. Technical Summary. Contribution of Working Group I to the Sixth Assessment Report of the Intergovernmental Panel on Climate Change, Climate Change 2021: The Physical Science Basis.

Jägermeyr, J., Müller, C., Ruane, A.C., Elliott, J., Balkovic, J., Castillo, O., Faye, B., Foster, I., Folberth, C., Franke, J.A., Fuchs, K., Guarin, J.R., Heinke, J., Hoogenboom, G., Iizumi, T., Jain, A.K., Kelly, D., Khabarov, N., Lange, S., Lin, T.-S., Liu, W., Mialyk, O., Minoli, S., Moyer, E.J., Okada, M., Phillips, M., Porter, C., Rabin, S.S., Scheer, C., Schneider, J.M., Schyns, J.F., Skalsky, R., Smerald, A., Stella, T., Stephens, H., Webber, H., Zabel, F., Rosenzweig, C., 2021. Climate impacts on global agriculture emerge earlier in new generation of climate and crop models. Nat. Food. https://doi.org/10.1038/s43016-021-00400-y.

Jeantet, A., Henine, H., Chaumont, C., Collet, L., Thirel, G., Tournebize, J., 2021. Robustness of a parsimonious subsurface drainage model at the French national scale. Hydrol. Earth Syst. Sci. 25, 5447–5471. https://doi.org/10.5194/hess-25-5447-2021.

Kimball, B.A., 2016. Crop responses to elevated CO2 and interactions with H2O, N, and temperature. Curr. Opin. Plant Biol. 31, 36–43. https://doi.org/10.1016/j.pbi.2016.03.006.

Laberdesque, M., Bessard Duparc, P., Soenen, B., Metais, P., Trochard, R., Le Bris, X., 2017. CHN: practical case of valorization of a dynamic crop model to estimate the number of available days for cultivation works, in: E-Agriculture Platform. FAO, Montpellier.

Lange, S., 2019. Trend-preserving bias adjustment and statistical downscaling with ISIMIP3BASD (v1.0). Geosci. Model Dev. 12, 3055–3070. https://doi.org/10.5194/gmd-12-3055-2019.

Le Bris X., Soenen B., Laberdesque M., Maunas M., Gouache D., Lorgeou J., Cohan J., Laurent F., Bouthier A., Garcia C. (2016) "CHN", a crop model to add value to phenotyping and approach genetic variation for RUE and WUE. Conference: Recent progress in drought tolerance: from genetics to modelling. At: Montpellier, France.

Liu, K., Harrison, M.T., Archontoulis, S.V., Huth, N., Yang, R., Liu, D.L., Yan, H., Meinke, H., Huber, I., Feng, P., Ibrahim, A., Zhang, Y., Tian, X., Zhou, M., 2021. Climate change shifts forward flowering and reduces crop waterlogging stress. Environ. Res. Lett. 16. https://doi.org/10.1088/1748-9326/ac1b5a.

Liu, B., Martre, P., Ewert, F., Porter, J.R., Challinor, A.J., Müller, C., Ruane, A.C., Waha, K., Thorburn, P.J., Aggarwal, P.K., Ahmed, M., Balkovič, J., Basso, B., Biernath, C., Bindi, M., Cammarano, D., De Sanctis, G., Dumont, B., Espadafor, M., Eyshi Rezaei, E., Ferrise, R., Garcia-Vila, M., Gayler, S., Gao, Y., Horan, H., Hoogenboom, G., Izaurralde, R.C., Jones, C.D., Kassie, B.T., Kersebaum, K.C., Klein, C., Koehler, A.-K., Maiorano, A., Minoli, S., Montesino San Martin, M., Naresh Kumar, S., Nendel, C., O'Leary, G.J., Palosuo, T., Priesack, E., Ripoche, D., Rötter, R. P., Semenov, M.A., Stöckle, C., Streck, T., Supit, I., Tao, F., Van der Velde, M., Wallach, D., Wang, E., Webber, H., Wolf, J., Xiao, L., Zhang, Z., Zhao, Z., Zhu, Y., Asseng, S., 2019. Global wheat production with 1.5 and 2.0°C above pre-industrial warming. Glob. Chang Biol. 25, 1428–1444. https://doi.org/10.1111/gcb.14542.

Liu, W., Ye, T., Jägermeyr, J., Müller, C., Chen, S., Liu, X., Shi, P., 2021. Future climate change significantly alters interannual wheat yield variability over half of harvested areas. Environ. Res. Lett. 16, 94045. https://doi.org/10.1088/1748-9326/ac1fbb.

Lobell, D.B., Schlenker, W., Costa-Roberts, J., 2011. Climate trends and global crop production since 1980. Science (1979) 333.

Madgwick, J.W., West, J.S., White, R.P., Semenov, M.A., Townsend, J.A., Turner, J.A., Fitt, B.D.L., 2011. Impacts of climate change on wheat anthesis and fusarium ear blight in the UK. Eur. J. Plant Pathol. 130, 117–131. https://doi.org/10.1007/s10658-010-9739-1.

McCuen, R., Zachary, K., Gillian, C.A., 2006. Evaluation of the Nash–Sutcliffe efficiency index. J. Hydrol. Eng. 11, 597–602. https://doi.org/10.1061/(ASCE)1084-0699(2006)11:6(597).

Muftuoglu, B., 2021. Russia steps up wheat exports to Algeria. Argus.

Nóia Júnior, Rogério de S., Deswarte, J.-C., Cohan, J.-P., Martre, P., van der Velde, M., Lecerf, R., Webber, H., Ewert, F., Ruane, A.C., Slafer, G.A., Asseng, S., 2023b. The extreme 2016 wheat yield failure in France. Glob. Chang Biol. 29, 3130–3146. https://doi.org/10.1111/gcb.16662.

Nóia Júnior, R. de S., Martre, P., Finger, R., van der Velde, M., Ben-Ari, T., Ewert, F., Webber, H., Ruane, A.C., Asseng, S., 2021. Extreme lows of wheat production in Brazil. Environ. Res. Lett. 16, 104025. https://doi.org/10.1088/1748-9326/ac26f3.

Nóia Júnior, Rogério de, S., Asseng, S., García-Vila, M., Liu, K., Stocca, V., dos Santos Vianna, M., Weber, T.K.D., Zhao, J., Palosuo, T., Harrison, M.T., 2023a. A call to action for global research on the implications of waterlogging for wheat growth and yield. Agric. Water Manag. 284, 108334. https://doi.org/10.1016/j.agwat.2023.108334.

Nóia Júnior, Rogério de, S., Olivier, L., Wallach, D., Mullens, E., Fraisse, C.W., Asseng, S., 2023. A simple procedure for a national wheat yield forecast. Eur. J. Agron. 148, 126868. https://doi.org/10.1016/J.EJA.2023.126868.

Nuttall, J.G., Barlow, K.M., Delahunty, A.J., Christy, B.P., O'Leary, G.J., 2018. Acute high temperature response in wheat. Agron. J. 110, 1296–1308. https://doi.org/10.2134/agronj2017.07.0392.

O'Neill, B.C., Carter, T.R., Ebi, K., Harrison, P.A., Kemp-Benedict, E., Kok, K., Kriegler, E., Preston, B.L., Riahi, K., Sillmann, J., van Ruijven, B.J., van Vuuren, D., Carlisle, D., Conde, C., Fuglestvedt, J., Green, C., Hasegawa, T., Leininger, J., Monteith, S., Pichs-Madruga, R., 2020. Achievements and needs for the climate change scenario framework. Nat. Clim. Change 10, 1074–1084. https://doi.org/10.1038/s41558-020-00952-0.

O'Neill, B.C., Tebaldi, C., van Vuuren, D.P., Eyring, V., Friedlingstein, P., Hurtt, G., Knutti, R., Kriegler, E., Lamarque, J.-F., Lowe, J., Meehl, G.A., Moss, R., Riahi, K., Sanderson, B.M., 2016. The scenario model intercomparison project (ScenarioMIP) for CMIP6. Geosci. Model Dev. 9, 3461–3482. https://doi.org/10.5194/gmd-9-3461-2016.

Paudel, D., Boogaard, H., de Wit, A., van der Velde, M., Claverie, M., Nisini, L., Janssen, S., Osinga, S., Athanasiadis, I.N., 2022. Machine learning for regional crop yield forecasting in Europe. Field Crops Res. 276, 108377. https://doi.org/10.1016/j.fcr.2021.108377.

Peel, M.C., Finlayson, B.L., McMahon, T.A., 2007. Updated world map of the Köppen-Geiger climate classification. Hydrol. Earth Syst. Sci. 11, 1633–1644. https://doi.org/10.5194/hess-11-1633-2007.

Pequeno, D.N.L., Hernández-Ochoa, I.M., Reynolds, M., Sonder, K., MoleroMilan, A., Robertson, R.D., Lopes, M.S., Xiong, W., Kropff, M., Asseng, S., 2021. Climate impact and adaptation to heat and drought stress of regional and global wheat production. Environ. Res. Lett. 16, 54070. https://doi.org/10.1088/1748-9326/abd970.

Ranasinghe, R., Ruane, A.C., Vautard, R., Arnell, N., Coppola, E., Cruz, F.A., Dessai, S., Islam, A.S., Rahimi, M., Carrascal, D.R., Sillmann, J., M.B. Sylla, C., Tebaldi, W., Wang, Zaaboul, R., 2021. Chapter 12: Climate change information for regional impact and for risk assessment. Climate Change 2021: The Physical Science Basis. Contribution of Working Group I to the Sixth Assessment Report of the Intergovernmental Panel on Climate Change 351–364.

Raymond, C., Horton, R.M., Zscheischler, J., Martius, O., AghaKouchak, A., Balch, J., Bowen, S.G., Camargo, S.J., Hess, J., Kornhuber, K., Oppenheimer, M., Ruane, A.C., Wahl, T., White, K., 2020. Understanding and managing connected extreme events. Nat. Clim. Change 10, 611–621. https://doi.org/10.1038/s41558-020-0790-4.

Reynolds, M.P., Slafer, G.A., Foulkes, J.M., Griffiths, S., Murchie, E.H., Carmo-Silva, E., Asseng, S., Chapman, S.C., Sawkins, M., Gwyn, J., Flavell, R.B., 2022. A wiring diagram to integrate physiological traits of wheat yield potential. Nat. Food 3, 318–324. https://doi.org/10.1038/s43016-022-00512-z.

Rezaei, E.E., Siebert, S., Hüging, H., Ewert, F., 2018. Climate change effect on wheat phenology depends on cultivar change. Sci. Rep. 8, 4891. https://doi.org/10.1038/s41598-018-23101-2.

Rötter, R.P., Hoffmann, M.P., Koch, M., Müller, C., 2018. Progress in modelling agricultural impacts of and adaptations to climate change. Curr. Opin. Plant Biol. 45, 255–261. https://doi.org/10.1016/j.pbi.2018.05.009.

Schauberger, B., Ben-Ari, T., Makowski, D., Kato, T., Kato, H., Ciais, P., 2018. Yield trends, variability and stagnation analysis of major crops in France over more than a century. Sci. Rep. 8, 16865. https://doi.org/10.1038/s41598-018-35351-1.

Schauberger, B., Makowski, D., Ben-Ari, T., Boé, J., Ciais, P., 2021. No historical evidence for increased vulnerability of French crop production to climatic hazards. Agric. Meteor. 306, 108453. https://doi.org/10.1016/j.agrformet.2021.108453.

Seneviratne, S., Zhang, X., Adnan, M., Badi, W., Dereczynski, C., Luca, A., Di, Ghosh, S., Iskandar, I., Kossin, J., Lewis, S., Otto, F., Pinto, I., Satoh, M., Vicente-Serrano, S.M., Wehner, M., Zhou, B., 2021. The physical science basis. In: Press, C.U. (Ed.), Sixth Assessment Report of the Intergovernmental Panel on Climate Change.

Simoes, A., 2022. The economic complexity observatory [WWW Document]. Workshops at the twenty-fifth AAAI conference on artificial intelligence. URL http://atlas.media.mit.edu/en/ (accessed 9.21.22).

Sweet, L., Müller, C., Anand, M., Zscheischler, J., 2023. Cross-validation strategy impacts the performance and interpretation of machine learning models. Artif. Intell. Earth Syst. 1–35. https://doi.org/10.1175/aies-d-23-0026.1.

te Beest, D.E., Shaw, M.W., Pietravalle, S., van den Bosch, F., 2009. A predictive model for early-warning of Septoria leaf blotch on winter wheat. Eur. J. Plant Pathol. 124, 413–425. https://doi.org/10.1007/s10658-009-9428-0.

Team, P.P., 2021. The POWER Project [WWW Document]. NASA Prediction of Worldwide Energy Resources. URL http://power.larc.nasa.gov/.

Tebaldi, C., Lobell, D., 2018. Estimated impacts of emission reductions on wheat and maize crops. Clim. Change 146, 533–545. https://doi.org/10.1007/s10584-015-1537-5.

Toreti, A., Deryng, D., Tubiello, F.N., Müller, C., Kimball, B.A., Moser, G., Boote, K., Asseng, S., Pugh, T.A.M., Vanuytrecht, E., Pleijel, H., Webber, H., Durand, J.-L., Dentener, F., Ceglar, A., Wang, X., Badeck, F., Lecerf, R., Wall, G.W., van den Berg, M., Hoegy, P., Lopez-Lozano, R., Zampieri, M., Galmarini, S., O'Leary, G.J., Manderscheid, R., Mencos Contreras, E., Rosenzweig, C., 2020. Narrowing uncertainties in the effects of elevated CO2 on crops. Nat. Food 1, 775–782. https://doi.org/10.1038/s43016-020-00195-4.

Trnka, M., Rötter, R.P., Ruiz-Ramos, M., Kersebaum, K.C., Olesen, J.E., Žalud, Z., Semenov, M.A., 2014. Adverse weather conditions for European wheat production will become more frequent with climate change. Nat. Clim. Change 4, 637–643. https://doi.org/10.1038/nclimate2242.

van der Velde, M., Lecerf, R., d'Andrimont, R., Ben-Ari, T., 2020. Chapter 8 - Assessing the France 2016 extreme wheat production loss—Evaluating our operational capacity to predict complex compound events, in: Sillmann, J., Sippel, S., Russo, S.B. T.-C.E. and T.I. for I. and R.A. (Eds.),. Elsevier, pp. 139–158. https://doi.org/10.1016/B978-0-12-814895-2.00009-4.

van der Velde, M., Tubiello, F.N., Vrieling, A., Bouraoui, F., 2012. Impacts of extreme weather on wheat and maize in France: evaluating regional crop simulations against observed data. Clim. Change 113, 751–765. https://doi.org/10.1007/s10584-011-0368-2.

Váry, Z., Mullins, E., McElwain, J.C., Doohan, F.M., 2015. The severity of wheat diseases increases when plants and pathogens are acclimatized to elevated carbon dioxide. Glob. Change Biol. 21, 2661–2669. https://doi.org/10.1111/gcb.12899.

Vogel, J., Rivoire, P., Deidda, C., Rahimi, L., Sauter, C.A., Tschumi, E., van der Wiel, K., Zhang, T., Zscheischler, J., 2021. Identifying meteorological drivers of extreme impacts: an application to simulated crop yields. Earth Syst. Dyn. 12, 151–172. https://doi.org/10.5194/esd-12-151-2021.

von Bloh, M., Nóia Júnior, R. de S., Wangerpohl, X., Saltık, A.O., Haller, V., Kaiser, L., Asseng, S., 2023. Machine learning for soybean yield forecasting in Brazil. Agric. Meteor. 341, 109670. https://doi.org/10.1016/j.agrformet.2023.109670.

Wallach, D., Goffinet, B., 1987. Mean squared error of prediction in models for studying ecological and agronomic systems. Biometrics 43, 561–573. https://doi.org/10.2307/2531995.

Webber, H., Ewert, F., Olesen, J.E., Müller, C., Fronzek, S., Ruane, A.C., Bourgault, M., Martre, P., Ababaei, B., Bindi, M., Ferrise, R., Finger, R., Fodor, N., Gabaldón-Leal, C., Gaiser, T., Jabloun, M., Kersebaum, K.-C., Lizaso, J.I., Lorite, I.J., Manceau, L., Moriondo, M., Nendel, C., Rodríguez, A., Ruiz-Ramos, M., Semenov, M. A., Siebert, S., Stella, T., Stratonovitch, P., Trombi, G., Wallach, D., 2018. Diverging importance of drought stress for maize and winter wheat in Europe. Nat. Commun. 9, 4249. https://doi.org/10.1038/s41467-018-06525-2.

Webber, H., Lischeid, G., Sommer, M., Finger, R., Nendel, C., Gaiser, T., Ewert, F., 2020. No perfect storm for crop yield failure in Germany. Environ. Res. Lett. 15, 104012. https://doi.org/10.1088/1748-9326/aba2a4.

West, J.S., Holdgate, S., Townsend, J.A., Edwards, S.G., Jennings, P., Fitt, B.D.L., 2012. Impacts of changing climate and agronomic factors on fusarium ear blight of wheat in the UK. Fungal Ecol. 5, 53–61. https://doi.org/10.1016/j.funeco.2011.03.003.

Xu, X., 2003. Effects of environmental conditions on the development of Fusarium ear blight BT - Epidemiology of Mycotoxin Producing Fungi: Under the aegis of COST Action 835 'Agriculturally Important Toxigenic Fungi 1998–2003', EU project (QLK 1-CT-1998–01380), in: Xu, X., Bailey, J.A., Cooke, B.M. (Eds.),. Springer Netherlands, Dordrecht, pp. 683–689. https://doi.org/10.1007/978-94-017-1452-5_3.

Zhang, D., Wang, Z., Jin, N., Gu, C., Chen, Y., Huang, Y., 2020. Evaluation of efficacy of fungicides for control of wheat fusarium head blight based on digital imaging. IEEE Access 8, 109876–109890. https://doi.org/10.1109/ACCESS.2020.3001652.

Zhao, C., Liu, B., Piao, S., Wang, X., Lobell, D.B., Huang, Y., Huang, M., Yao, Y., Bassu, S., Ciais, P., Durand, J.-L., Elliott, J., Ewert, F., Janssens, I.A., Li, T., Lin, E., Liu, Q., Martre, P., Müller, C., Peng, S., Peñuelas, J., Ruane, A.C., Wallach, D., Wang, T., Wu, D., Liu, Z., Zhu, Y., Zhu, Z., Asseng, S., 2017. Temperature increase reduces global yields of major crops in four independent estimates, 9326 LP – 9331 Proc. Natl. Acad. Sci. 114. https://doi.org/10.1073/pnas.1701762114.